

PCCP

Accepted Manuscript



This is an *Accepted Manuscript*, which has been through the Royal Society of Chemistry peer review process and has been accepted for publication.

Accepted Manuscripts are published online shortly after acceptance, before technical editing, formatting and proof reading. Using this free service, authors can make their results available to the community, in citable form, before we publish the edited article. We will replace this *Accepted Manuscript* with the edited and formatted *Advance Article* as soon as it is available.

You can find more information about *Accepted Manuscripts* in the [Information for Authors](#).

Please note that technical editing may introduce minor changes to the text and/or graphics, which may alter content. The journal's standard [Terms & Conditions](#) and the [Ethical guidelines](#) still apply. In no event shall the Royal Society of Chemistry be held responsible for any errors or omissions in this *Accepted Manuscript* or any consequences arising from the use of any information it contains.

ARTICLE

Label-Free Detection of DNA Single-Base Mismatches using a Simple Reflectance-Based Optical Technique

Cite this: DOI: 10.1039/x0xx00000x

G. Nava*,^a E. Ceccarello*,^a F. Giavazzi,^a M. Salina,^b F. Damin^c, M. Chiari^c, M. Buscaglia^a, T. Bellini,^a and G. Zanchetta^aReceived 00th January 2012,
Accepted 00th January 2012

DOI: 10.1039/x0xx00000x

www.rsc.org/

Rapid and quantitative detection of the binding of nucleic acids to surface-immobilized probes remains a challenge in many biomedical applications. We investigated the hybridization of a set of fully complementary and defected 12-base long DNA oligomers by using Reflective Phantom Interface (RPI), a recently developed multiplexed label-free detection technique. Based on the simple measurement of reflected light intensity, this technology enables to quantify the hybridization directly as it occurs on the surface with a sensitivity of 10 pg/mm². We found a strong effect of single-base mismatches and of their location on hybridization kinetics and equilibrium binding. In line with previous studies, we find that DNA-DNA binding is weaker on a surface than is in the bulk. Our data indicate that this effect is a consequence of weak nonspecific binding of the probes to the surface.

Introduction

The hybridization process, by which nucleic acids chains recognize and selectively bind to complementary strands, is at the basis of a whole range of biological processes.^[1] Furthermore, simple and robust detection and discrimination of nucleic acids sequences is of critical importance for various biomedical applications, ranging from gene expression profiling to determination of single point mutations to quantification of microRNAs as possible biomarkers for diseases.^[2,3,4] Along with biomedical investigation, the research aiming at the exploitation of DNA to realize nanostructures like scaffolds, drug carriers, or nanomachines - in brief DNA nanotechnology^[5] - is gaining increasing interest and critically relies on accurate detection, modelling and control of hybridization process.

In recent years, DNA microarrays, based on the recognition and hybridization of target sequences by surface immobilized single-stranded DNA (ssDNA) probes, have reached considerable success and widespread use for their versatility and massive data generation^[6]. However, conventional detection methods based on fluorescent emission of labelled targets fail to quantitatively assess concentrations and binding energies, which affects their reliability and reproducibility. Therefore, label-free methods enabling quantitative detection of DNA binding while preserving multiplexing, scalability and cheapness, appear of general interest^[3].

Here we apply for the first time to DNA-DNA recognition a recently proposed label-free optical technique, Reflective Phantom Interface (RPI).^[7,8,9,10] RPI is based on measuring the increase of reflected light intensity upon mass adsorption on a surface with extremely low initial reflectivity, which thus yields a high signal-to-noise ratio. We realize this condition by using a fluorinated material iso-refractive to water as sensing substrate. Changes in reflectance allow the quantification of small variations in the amount of molecules at the interface, such as those produced by the binding of ligand target molecules to surface-immobilized receptor probes. This approach requires a particularly simple measuring procedure and experimental setup^[8]. We measure kinetic and equilibrium binding constants upon hybridization of probe and target DNA 12-mers, demonstrating a detection sensitivity of about 10 pg/mm² of oligomers bound to the surface. The effect of a single nucleotide mismatch in pairing sequence is easily discriminated and quantified.

In line with other observations of surface hybridization, we find a binding strength weaker than expected in the bulk. Our data enable discriminating among the various potential causes of such weakening.

Experimental

Substrate preparation

The fluorinated material used in this study (Hyflon AD60, Solvay Specialty Polymers, Italy) is an optically transparent,

amorphous, glassy copolymer of tetrafluoroethylene and 2,2,4-trifluoro-5-trifluoromethoxy-1,3-dioxole containing 60 mol% of the cyclic comonomer, with a refractive index ($n_{\text{Hyflon}} \approx 1.327$) very close to the typical buffered water value ($n_{\text{TrisHCl}} \approx 1.335$ in our experimental conditions), yielding a “background” reflectivity $R_0 \lesssim 10^{-5}$. The bulk material was machined and mechanically lapped to obtain prisms with optical quality faces. The prisms were cleaned with distilled water and plasma treatment and then immersed for 30 min in a water solution of ammonium sulfate at 20% (wt/vol) saturation, containing 1% wt/vol of a different polymer, copoly(DMA-NAS-MAPS) [11], that serves the two purposes of coating of the Hyflon surface and of providing a few nm-thick scaffold for the grafting of aminated molecules. The coated prisms were then rinsed with water and dried under vacuum at 80 °C. The estimated roughness of the substrate, between 0.1 and 1 μm , did not change upon such treatments, while its reflectivity only slightly increased - around 25% - without substantially affecting RPI sensitivity.

DNA sequences

By taking advantage of the multiplexing capacity of RPI, we prepared surfaces with multiple spots carrying various 12-base long DNA oligomers that interact with the same target sequence present in solution. Specifically, the target sequence is 5'-ACGACAGTCCTG-3' (12T) while the probe sequences are: 12FC: NH₂-5'-CAGGACTGTCGT-3', complementary to 12T; 12CM: NH₂-5'-CAGGAATGTCGT-3', with one central mismatch (underlined); 12TM3: NH₂-5'-CAGGACTGTCGA-3', with one mismatch at the 3' terminal; 12TM5: NH₂-5'-AAGGACTGTCGT-3', with one mismatch at the 5' terminal.

To test the effect of the distance from the surface, we also studied sequences with polyA spacers on the tethered end (A_n-12FC: NH₂-5'-(A)_nCAGGACTGTCGT-3', n = 6,12).

Negative controls consisted of a sequence completely unrelated to 12FC, 23CTRL:

NH₂-5'-GCCACCTATAAGGTAAAAGTGA-3'.

All sequences were purchased from Integrated DNA Technologies, with HPLC purification.

DNA Immobilization

After coating with the copolymer, the sensing surface of the prism was functionalized with the aminated DNA sequences, spotted with an automated noncontact dispensing system (sciFLEXARRAYERS5; Scienion AG).

The DNA sequences were spotted in droplets at concentrations ranging from $c_s = 0.625 \mu\text{M}$ to $c_s = 20 \mu\text{M}$ in Tris-HCl buffer pH 8 to obtain different surface probe densities. Moreover, each spot had multiple replicates to provide better statistics. The prisms were then incubated overnight in a humid chamber at room temperature. The spotted prisms were immersed in a 50 mM ethanolamine solution (Tris HCl 10 mM, NaCl 150 mM, pH 8) for 30 minutes, rinsed with distilled water and dried before use. No further surface passivation was found necessary.

Hybridization experiments and data analysis

Details about the RPI optical setup can be found in [7]. The spotted prism was inserted into a standard glass cuvette and immersed in an incubation buffer consisting of Tris-HCl 10 mM, NaN₃ 0.02%, pH 8. Ionic strength was adjusted between 60 and 160 mM with added NaCl. The cuvette was kept at constant temperature through a thermalized holder.

The sensing surface was illuminated by a LED source (HLMP-ED18-UX000; Avago Technologies) emitting at 450 nm - with a spectral half width of 17 nm. Reflected light was collected by a CCD camera (Stingray F-145B/C; Allied Technology). We acquired time-lapse videos of the surface with rate of 1 frame per second, averaging every 5 consecutive frames. For each averaged frame, we extracted the intensity reflected by each spot and by its corresponding corona, as shown in Fig. 1 (inset picture). We then averaged the intensities of spots corresponding to identical conditions (probe type and spotting concentration), and of their coronas. Fig. 1 shows such intensities u (spots) and u_{cor} (coronas) over time for 12FC probes.

Keeping the cell at 33 °C, we introduced in the cuvette, at given times (t_c), increasing amounts of 12T, to produce a stepwise increase of target concentration, from $c_T = 0.3 \text{ nM}$ to $c_T = 3 \mu\text{M}$, as marked by the shadings of Fig. 1. After each increment in c_T , the reflected intensity had a transient response corresponding to the DNA targets adhering to the surface.

Details about the analysis of reflectivity data can be found in the Electronic Supplementary Information. In brief, the mean reflected intensity can be converted into the surface density of the mass present at the interface, σ , by describing the reflectance of a multi-layered structure [7]. Specifically,

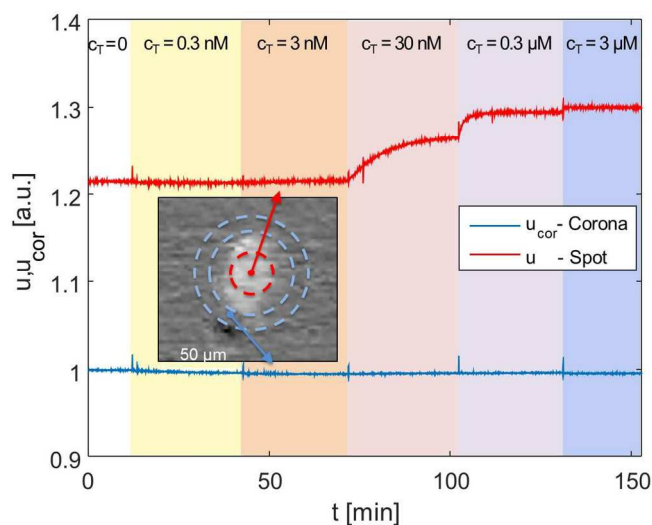


Figure 1 Example of the reflected intensity averaged over the area of a single spot ($u(t)$, red line) and over the surrounding corona ($u_{\text{cor}}(t)$, blue line) plotted as a function of time for 12T sequence adhering to immobilized 12FC. At $t = 13, 42, 75, 103$ and 133 min target sequences were added in the solution so to increase step-wise their overall concentration from 0 to $3 \mu\text{M}$. The inset shows an optical image of a typical spot and highlights the regions identified as spot and corona.

$$\sigma = \sigma_0 \sqrt{u/u_0 - 1} \quad (1)$$

where u_0 is the intensity reflected by the bare surface ($u_{cor}/u_0 \approx 1.25$ in the experimental conditions here employed [8]). $\sigma_0 \approx 4.9 \text{ ng/mm}^2$ is a constant that depends on the system parameters and represents the surface density yielding a twofold increase of the brightness relative to u_0 .

Results and discussion

Hybridization measurements by RPI

The neat growth of u that follows the injections of target sequences, displayed in Fig. 1, is a clean indication that RPI can effectively sense the binding process. Fig. 2a shows the surface density of bound target, $\Delta\sigma = \sigma - \sigma(t=0)$ (Eq. 1) for the four different probes with the same length averaged over 4 spots each, plus the control probe which shows no sign of aspecific binding. The spots were produced with equal spotting concentration c_s on the same chip. Therefore, the injection of 12T is the same for each probe and equal to the one reported in Fig. 1. Each increase of the target surface density $\Delta\sigma$ after the injection time t_c , can be well fitted with a single exponential function (shown in Fig. 2a as black thin lines):

$$\Delta\sigma(t) = \Delta\sigma_c - \Delta\Delta\sigma \exp[-(t - t_c)/\tau_c] \quad (2)$$

where $\Delta\Delta\sigma$ is the increment in the mass density of the spot associated to the increment of c_T , while $\Delta\sigma_c$ and τ_c represent the equilibrium plateau value and the characteristic timescale of the process at a given c_T , respectively.

Fig. 2b shows the dependence of the equilibrium surface concentration $\Delta\sigma_c$ on c_T , indicating growth and saturation. This behaviour suggests a first order adsorption mechanism. Indeed, $\Delta\sigma_c(c_T)$ is well fitted by the expression expected for Langmuir adsorption isotherms [12]:

$$\Delta\sigma_c(c_T) = \Delta\sigma_{sat} c_T / (c_T + K_{diss}) \quad (3)$$

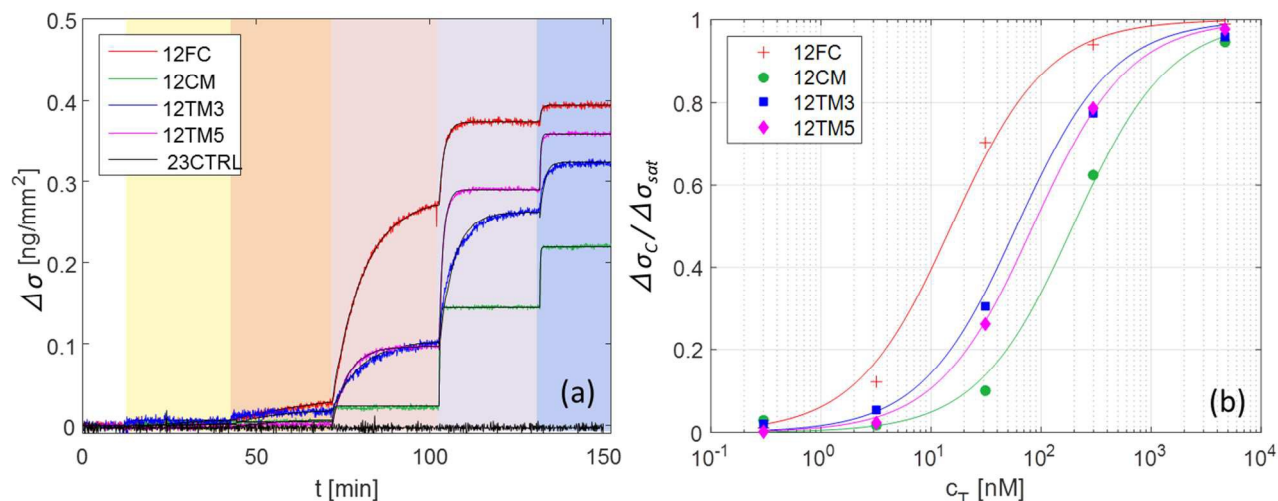


Figure 2 Increase of the surface density of bound target strand 12T, upon hybridization to different probes, for increasing concentration of 12T in solution (ionic strength $I_{Na} = 160 \text{ mM}$, $T = 33 \text{ }^\circ\text{C}$, $c_s = 6.25 \text{ } \mu\text{M}$). (a) Surface density signal averaged over 4 spots each; color shading for 12T addition is the same as in Fig. 1., black lines are fits with Eq. 2. (b) Fraction of occupied binding sites for the 4 DNA probes upon increase of target concentration; lines are fits with Langmuir model Eq. 3.

where $\Delta\sigma_{sat}$ corresponds to the target mass density on the spots when all available probes have been saturated by target strands; K_{diss} is the thermodynamic dissociation constant of the hybridization process and corresponds to the concentration at which $\Delta\sigma_c(c_T)$ has an inflection point. Table 1 reports the values for K_{diss} obtained from the fits in Fig. 2b.

In all linear two-state processes, $K_{diss} = k_{off}/k_{on}$, with k_{on} and k_{off} the association and dissociation kinetic coefficients, respectively. The measured τ_c depends on such coefficients as [12]:

$$\frac{1}{\tau_c} = k_{off} + c_T k_{on} \quad (4)$$

According to Eq. 4, in the limit of low concentration when $c_T \ll K_{diss}$, the timescale of the relaxation is determined by k_{off} . Conversely, when $c_T \gg K_{diss}$ the measured kinetics is dominated by k_{on} . Thus both kinetic coefficients could be in principle determined by studying the intercept and slope of $1/\tau_c$. However, at the lowest c_T the fitting procedure of $\Delta\sigma(t)$ has a large uncertainty on both $\Delta\sigma_c$ and τ_c , while their ratio $\Delta\sigma_c/\tau_c$ is much better determined, since it corresponds to the slope of $\Delta\sigma(t)$ right after the injection of targets. Accordingly, we can obtain a more convenient and robust way to estimate k_{on} from the experimental data by combining Eqs. 3 and 4 into:

$$\frac{\Delta\sigma_c}{\Delta\sigma_{sat}\tau_c} = c_T k_{on}. \quad (5)$$

The corresponding data and fit procedure are shown in Fig. 3. The values obtained for k_{on} are reported in Table 1, which also shows the values of k_{off} determined from K_{diss} and k_{on} .

Sequence	k_{on} ($\text{sec}^{-1}\text{nM}^{-1}$)	k_{off} (sec^{-1})	K_{diss} (nM)	$K_{\text{diss,L}}$ (nM)	$K_{\text{diss,NN}}$ (nM)
12FC	$1.79 \cdot 10^{-5}$	$2.6 \cdot 10^{-4}$	14.5	7	0.12
12TM3	$2.02 \cdot 10^{-5}$	$1.4 \cdot 10^{-3}$	68.8	30	0.30
12TM5	$1.6 \cdot 10^{-5}$	$1.3 \cdot 10^{-3}$	84.4	40	0.89
12CM	$14.1 \cdot 10^{-5}$	$2.63 \cdot 10^{-2}$	187.1	228	12.9

Table 1. Kinetic and equilibrium coefficients for 12T hybridization to various probe strands. k_{on} , k_{off} , K_{diss} : values extracted from data in Figs. 2 and 3. $K_{\text{diss,L}}$: dissociation constants extrapolated for low probe surface density (average value for 12CM). $K_{\text{diss,NN}}$: reference values calculated according to the standard nearest-neighbour model [13,14].

Hybridization of sequences with single nucleotide mismatches

The traces shown in Fig. 2a display clear differences in the hybridization of the target strand to the four probes. The complete hybridization of 12FC leads to the largest σ increment when $c_T = 30$ nM, while the sequences with a mismatch pair most significantly to the surface probes when $c_T = 300$ nM. This difference corresponds to different binding coefficient, as reported in Table 1. K_{diss} markedly increases when mismatches are present in the sequence, of about 5 times if the defect is at the sequence terminal, and of about 13 times in the case of a central defect. The dependence of the thermodynamic stability of the duplexes on the mismatch position along the oligomer strands is a well-known property of nucleic acids [15,16]. In Table 1, we report the values of $K_{\text{diss,NN}}$, the dissociation coefficient computed for solution hybridization of the same sequences on the basis of the well-established nearest-neighbour model [13,14]. The strong dependence of the effect of a single mismatch on the position is confirmed by the computed values $K_{\text{diss,NN}}$, which show the same scaling of K_{diss} with the probe sequence. However, all the computed values are much lower than those measured via RPI, indicating that bulk hybridization is stronger than surface hybridization, a phenomenon often observed in analogous experiments and discussed in a later section.

The kinetic behaviour is also distinctly different in the four systems. A marked dependence of the hybridization kinetics on the mismatch position has also been previously reported [17]. In the context of the experiments described here, this effect is

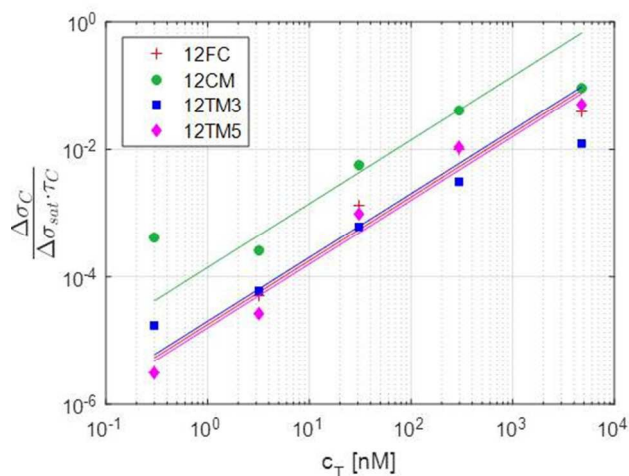


Figure 3 The initial slope of exponential fit shown in Fig. 2a provides an evaluation of kinetic association constant through Eq. 5

particularly striking in the case of the hybridization with a central mismatch, in which binding takes place in a much shorter time than in the other cases. The quantitative analysis of such behaviour, Figure 3 and Table 1, reveals that k_{off} is much more sensitive to mismatches than k_{on} . A pronounced increase of k_{on} is only observed for the central mismatch, in contrast with solution behaviour of shorter oligomers [18]; however, also in this case, the increase of k_{off} is larger. This appears reasonable, since k_{on} mainly reflects the height of the entropic barrier that the two strands have to overcome to get close enough to each other to enable the formation of the duplex through the enthalpic gain of stacking and pairing [19]. Accordingly, k_{on} is expected to be much less sensitive to the quality of the pairing than k_{off} , which is instead mainly determined by the enthalpy needed to unbind the two strands.

Effect of probe surface density and of ionic strength

The hybridization curves of Fig. 2 were measured on spots of surface-immobilized probes that were all produced with equal c_S . We attribute the differences in the $\Delta\sigma_{\text{sat}}$ measured with the different probes to minor experimental differences in the spotting process. However, to explore the possible effects of probe surface crowding, we performed measurements analogous to those in Fig. 2 at different spotting concentrations, ranging from $c_S = 0.6 \mu\text{M}$ to $c_S = 25 \mu\text{M}$, for all the different probes. Such concentrations correspond to probe surface densities in the range $3\text{-}10 \cdot 10^{10}$ molecules/ mm^2 , as assessed from the measured $\Delta\sigma_{\text{sat}}$ values (see Fig. S3 in ESI). The highest density of this range corresponds to about 1 probe per 10 nm^2 , a condition where the mean distance between neighbouring probes is in the order of their length.

In Fig. 4 we plot K_{diss} , determined by fitting $\Delta\sigma_C(c_T)$ with Langmuir isotherms as in Fig. 2b; $\Delta\sigma_C(c_T)$ is measured in spots having different surface concentration of active probes, as expressed by $\Delta\sigma_{\text{sat}}$. While no clear trend is visible in the hybridization of 12CM, in the case of perfect pairing or terminal mismatches we can observe a slight but monotonic

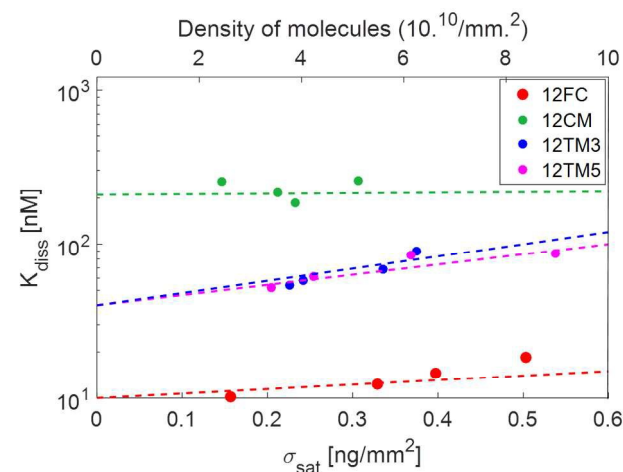


Figure 4 Dissociation constant as a function of surface density (bottom axis) and number density of molecules (top axis) for the various probes. Dashed lines indicate extrapolation to vanishing surface density (except for 12CM, where the average value is shown).

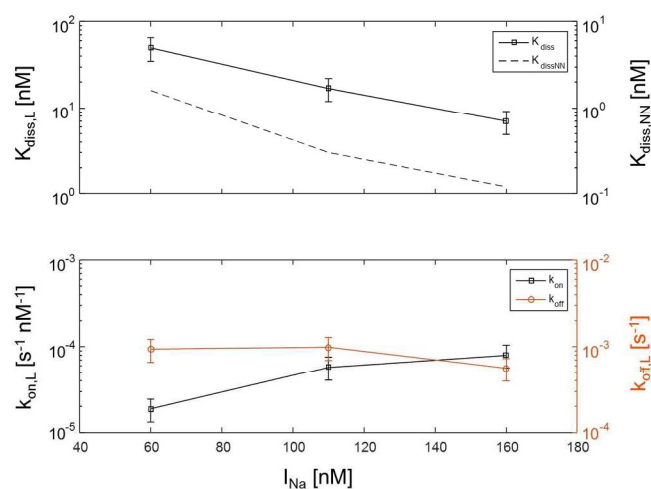


Figure 5 Dependence of thermodynamic constants for 12FC-12T binding on the ionic strength I_{Na} . (a) The extrapolated dissociation constant $K_{diss,L}$ is compared to the expected solution behaviour $K_{diss,NN}$ (right axis, dashed line). (b) Kinetic constants - extrapolated for low surface density - k_{on} (left axis) and k_{off} (right axis).

dependence, suggesting that binding may be weakened by crowding at the probe surface [20]. Indeed, when the probes are at distance of contact to each other as is for the densest spots, it appears reasonable that hybridization is affected by their mutual electrostatic or steric hindrance. To take into account these effects, we report in Table 1 the values of $K_{diss,L}$, the equilibrium coefficients obtained by extrapolating the measured K_{diss} to limiting low probe concentrations along the lines in Fig. 4. Although these values have larger intrinsic uncertainty than K_{diss} , it is quite clear that their values are still much higher than those for solution hybridization.

Ionic strength I_{Na} is very well known to significantly affect hybridization in the bulk. To explore analogous effects in surface hybridization, we performed measurements with the 12FC probes changing concentration of Na^+ ions between 60 mM and 160 mM. In Fig. 5a, we compare measured values of dissociation constant $K_{diss,L}$ with the expected solution coefficients $K_{diss,NN}$, finding a similar dependence on ionic strength. Fig. 5b shows the I_{Na} dependence of the kinetic coefficients. Data indicate that that upon increasing I_{Na} , the strengthening of the duplex binding is mainly due to the increase of k_{on} , while k_{off} is only weakly affected, in agreement with previous single molecule measurements both in solution and at surface [18,21].

How does surface affect binding?

Hybridization at the surface, as measured with RPI, is weaker than its counterpart in the bulk. The ratio between K_{diss} and $K_{diss,NN}$ ranges from about 15 - for a central pairing defect - to about 100 for the fully complementary binding.

Systematic and relevant differences in the values of binding affinities and hybridization kinetics of DNA oligomers when measured in solution vs. on a sensor surface have been documented in a number of previous articles (see e.g. [2,22] and references therein). Most of these studies have focused on immobilized oligomeric probe interacting with long target

strand, much longer than those considered here. In that case a major role is played by the molecular crowding at the surface, which follows the binding itself [23]. However, important effects on affinities and kinetics were also found for oligomeric targets with length comparable to the ones we studied here [22,24,25].

In line with what we observe with RPI, previous investigations have found that even at low probe density - where crowding plays no role - and at large ionic strengths - where electrostatics is screened - binding can be orders of magnitude weaker than in solution, while the interaction is still well described by a Langmuir isotherm [26]. Other studies have shown that the nature of the surface - hydrophobic vs. hydrophilic - also plays a complex role in the hybridization of DNA [27,28].

Overall, the possible causes of the weakening of the hybridization free energy at surface can be classified into two main groups: (i) effects due to target repulsion by the surface, and (ii) effects due to the competition of probe-target binding with nonspecific interactions of probe and/or target.

For what concerns point (i), target repulsion by the surface can rise from electrostatic interaction with the surface-bound probes, targets or other ions. The data described above indicate that electrostatic effects should not be considered as the main origin of surface-induced duplex weakening: the ionic strength dependence is as expected in solution hybridization, and the probe density, which contributes to the surface charge density, has only a mild effect. It is also worth noticing that the roughly exponential dependence expressed by the lines in Fig. 4 agrees with predictions based on surface electrostatic repulsion [23], confirming that electrostatic repulsion is indeed detected, but with minor effects.

Alternatively, repulsion could be ascribed to the steric constraints imposed by the thin 3D polymeric matrix (around 85% of its volume is occupied by water), to which the probes are grafted. The targets might have to navigate into a molecularly crowded environment that limits the accessibility of the probes. This is expected to directly affect the kinetics of binding and unbinding. However, less obvious is the effect on the equilibrium of the interaction. As in the case of the electrostatic repulsion [26], the main effect can be described as an uneven partitioning of the targets between the bulk solution and the surface layer of immobilized probes. In this case, the concentration of target strands close to the surface $c_{T,S}$ is reduced with respect to the bulk concentration $c_{T,V}$ by $c_{T,S}/c_{T,V} = \exp(-\mu_S/k_B T)$, where μ_S is the chemical potential increment at the surface, that is the work required to transfer one target molecule from bulk to surface. This means that the apparent binding and kinetic coefficients measured by controlling $c_{T,V}$, are also modified by the same factor controlling the surface concentration. Since such a factor is in our case of the order of 100, this simple evaluation suggests a significant repulsive barrier of the order of $5 k_B T$. Should this barrier be interpreted as a reduction of the conformational volume Ω of the targets in the proximity of the probes (i.e. $\mu_S = k_B T \ln(\Omega_{vol}/\Omega_{surf})$), it would lead to the unrealistic conclusion that the phase space within the matrix is 100 times

smaller than in solution. To further test this notion, we checked the effect of placing a molecular spacer between the copolymer coating and the probe sequence to increase the distance of the docking sites from the coating polymer branches [29]. This was done by inserting a 6- or 12-bases long polyA tract on the tethered side of the 12FC probe. Rather than facilitating the hybridization, distancing the probe from the surface produced a slight decrease of the estimated affinities (Fig. S4 in ESI), likely due to enhanced crowding of the probes. Therefore, neither the electrostatic nor the steric repulsion of the polymer coating seem to provide a plausible origin of the observed weakening of the hybridization strength at the surface.

As anticipated in point (ii), an alternative explanation of the reduced binding strength is the presence of other attractive interactions that compete with the probe-target interaction. These mainly include forms of nonspecific adhesion of the probes on the polymer support or sensor surface they are attached to. Surface-target interaction may also be present, but the identical nature of probes and targets suggests that these interactions, if present, are much more relevant for the probes, constrained to a continuous contact with the surface by their chemical bonds. Indeed, no sign of nonspecific adhesion of target strands was ever detected outside the functionalized spots. In principle, probe-probe interactions could also be present, as discussed in the context of different experiments [2]. Complex probe-probe interactions mediated by targets have also been suggested [26]. However, the weak dependence of binding strength on probe concentration that we observe suggests that no form of probe-probe interaction is actually playing a relevant role in our case, and thus points to probe-surface effects.

The competitive effect of probe-surface interaction can be estimated by a simple set of combined equilibrium equations:

$$\begin{aligned} p \cdot t_0 &= K_{diss,V} \cdot pt \\ p \cdot s_0 &= K_S \cdot ps \\ p_T &= p + pt + ps \end{aligned} \quad (6)$$

where all quantities are measured in molar concentrations. t_0 is the solution concentration of target sequences, s_0 is the effective concentration of surface probe binding sites, i.e. surface sites able to transiently bind a portion of the probe chain. p_T , p , pt and ps are the total, free, target-bound and surface-bound concentrations of probes, respectively. $K_{diss,V}$ and K_S are the binding coefficients of probes and targets in solution and of probes to surface, respectively. The order of magnitude of s_0 can be estimated considering that the portion of surface interacting with one probe strand is limited to that reached by the probe as it fluctuates about its fixed connection point to the surface. Thus we can assume that there is at least one surface-docking site within the hemispherical volume V that the probe can span, $V \approx 2\pi\ell^3/3$, with $\ell \approx 3$ nm being the length of the probe. From this estimate it follows that $s_0 \geq 10$ mM. Ignoring the surface contribution, one would write a similar set of equations as Eq. 6 (without the second equation) and with an effective probe-target dissociation coefficient $K_{diss,E}$, weakened

by the competition with the surface. According to this simple model, $K_{diss,E} = K_{diss,V}(1 + s_0/K_S)$. To obtain the factor of 100 suggested by the experiments, we would need a surface binding coefficient $K_S \approx s_0/100$. This estimate yields $K_S \geq 100$ μ M, a figure corresponding to a very weak interaction strength, well in the range of nonspecific binding coefficients. The fact that weak nonspecific interactions with the surface can have such a significant effect on the strong and selective DNA hybridization mechanism, can thus be understood as ultimately due to the low entropic penalty associated to the adhesion of the probe to the surface to which it is already chemically connected. This description incorporates the notion that the probes are flexible and that hybridization is distributed along the whole chain, features specific to nucleic acids. Thus, in the presence of nonspecific interaction with the surface, the flexible probes can stick on it in a variety of patterns, all incompatible with the complete formation of a duplex, with which they thus compete [30]. This marks a difference with protein ligand-receptor interactions occurring at a surface, which typically maintain the affinity they have in solution.

Finally, we remark that a competition mechanism in surface binding appears to be consistent with both the lack of effects following the insertion of poly-A spacers, and with the observed kinetics. It is reasonable to expect that a competition with nonspecific binding should affect the association kinetics (k_{on}), while leaving k_{off} less affected.

Sensitivity of RPI for DNA hybridization

Sensitivity represents one of the key elements for the performances of DNA detection techniques. Limit of detection given in terms of molar concentration of target in solution clearly depends on the strength of the interaction. Rather, a more relevant quantity for a surface-based method is the mass sensitivity. The minimum amount of target molecules that can be detected on the surface of the RPI system presented here was estimated considering the fluctuation of the signal. The limit of detection, corresponding to 3 times the standard deviation, is about 10 pg/mm², which is equivalent to $\sim 2 \times 10^9$ molecules/mm² or $\sim 2 \times 10^6$ molecules/spot for the dodecamers investigated.

This value is comparable to those typically reported for Surface Plasmon Resonance [31,32] and others among the most sensitive label-free techniques [3,33].

As for fluorescence-based methods, reported sensitivities are one to two orders of magnitude higher [34]; however, it is often difficult to quantitatively relate fluorescence intensity to the amount of molecules actually captured on the surface [35], also for the limitations intrinsic to fluorescence emission like bleaching and quenching [36]. Thus, the quantification of genetic expression levels by fluorescence requires complicated procedures, which may affect the reproducibility of the results [37]. Conversely, despite the lower sensitivity, the RPI method offers a direct quantification of target concentration with minimum sample preparation and short time-to-result.

Moreover, the direct access to the binding curves enables to exploit the large difference of hybridization kinetics observed between the fully complementary sequence and that presenting a central single-base mutation. Remarkably, as shown in Figure 2a, in the target concentration range between 30 nM and 300 nM, the binding curves for the 12CM sequence are much faster and have lower amplitude than those for 12FC. This result suggests that considering the time slope of the surface binding measured by RPI, a single-base mutation can be revealed in only a few minutes without washing steps or addition of labelling reagents.

Conclusions

We have applied RPI, a novel label-free optical technique based on surface reflectance, to the detection and quantification of DNA oligomers hybridization. We find good sensitivity to binding events and high specificity for the presence and position of pairing defects.

The major points of this study are:

(i) The real-time access to the hybridization process provided by RPI allows for the rapid and robust discrimination of single-nucleotide mismatches, based on both kinetic and equilibrium properties of the binding events.

(ii) We addressed the origin of the weakening of the hybridization strength for surface-immobilized DNA, often observed in the literature. We interpret and model this effect as the result of very weak, non-specific probe-surface interactions.

The simplicity inherent to the RPI technology, combined to its multiplexing capability, can provide easy access to the investigation of DNA-DNA interactions occurring at surfaces and to the detection of specific sequences for diagnostic purposes.

Acknowledgements

We acknowledge support from MIUR grant “Building Materials with DNA bricks” (2010LKE4CC) and from EU (NAPES Project – NMP-2013-SMALL-7, Project no. 604241). We thank Solvay Solexis for kindly providing the Hyflon substrate and A. Baldo and S. Villa for experimental support. We also gratefully acknowledge useful discussions with R. Asselta, E. Paraboschi, G. Tagliabue and C. Battaglia and comments by referees which helped to improve the manuscript.

Notes and references

^a Dipartimento di Biotecnologie Mediche e Medicina Traslazionale, Università degli Studi di Milano, via Fratelli Cervi 93, 20090 Segrate, Milano, Italy.

Email: giuliano.zanchetta@unimi.it

^b Proxentia S.r.l., 20135 Milano, Italy.

^c Istituto di Chimica del Riconoscimento Molecolare (ICRM), C.N.R., Via Mario Bianco 9, 20131 Milano, Italy.

* These authors contributed equally to this work.

Electronic Supplementary Information (ESI) available: Details about data analysis, effect of spotting concentration on probe surface density, effect of polyA spacers on affinity estimates. See DOI: 10.1039/b000000x/

- 1 C. R. Calladine, H. R. Drew, B. F. Luisi, A. A. Travers, C.R.C., H.R.D., B.F.L. and A.A.T., *Understanding DNA*, Elsevier, 2004.
- 2 A. N. Rao and D. W. Grainger, *Biomater. Sci.*, 2014, **2**, 436–471.
- 3 E. Ozkumur, S. Ahn, A. Yalçın, C. A. Lopez, E. Cevik, R. J. Irani, C. DeLisi, M. Chiari and M. S. Unlü, *Biosens. Bioelectron.*, 2010, **25**, 1789–95.
- 4 W. Filipowicz, S. N. Bhattacharyya and N. Sonenberg, *Nat. Rev. Genet.*, 2008, **9**, 102–14.
- 5 T. Bellini, R. Cerbino and G. Zanchetta, *Top. Curr. Chem.*, 2012, **318**, 225–79.
- 6 F. TELES and L. FONSECA, *Talanta*, 2008, **77**, 606–623.
- 7 F. Giavazzi, M. Salina, R. Cerbino, M. Bassi, D. Proserpi, E. Ceccarello, F. Damin, L. Sola, M. Rusnati, M. Chiari, B. Chini, T. Bellini and M. Buscaglia, *Proc. Natl. Acad. Sci. U. S. A.*, 2013, **110**, 9350–5.
- 8 F. Giavazzi, M. Salina, E. Ceccarello, A. Ilacqua, F. Damin, L. Sola, M. Chiari, B. Chini, R. Cerbino, T. Bellini and M. Buscaglia, *Biosens. Bioelectron.*, 2014, **58**, 395–402.
- 9 M. Salina, F. Giavazzi, R. Lanfranco, E. Ceccarello, L. Sola, M. Chiari, B. Chini, R. Cerbino, T. Bellini and M. Buscaglia, *Biosens. Bioelectron.*, 2015, **74**, 539–545.
- 10 M. Salina, F. Giavazzi, E. Ceccarello, F. Damin, M. Chiari, M. Ciuffo, G. P. Accotto and M. Buscaglia, *Sensors Actuators B Chem.*, 2016, **223**, 957–962.
- 11 G. Pirri, F. Damin, M. Chiari, E. Bontempi and L. E. Depero, *Anal. Chem.*, 2004, **76**, 1352–8.
- 12 P. Atkins and J. de Paula, *Physical Chemistry*, W. H. Freeman, 2009.
- 13 J. SantaLucia, *Proc. Natl. Acad. Sci.*, 1998, **95**, 1460–1465.
- 14 R. Owczarzy, Y. You, B. G. Moreira, J. A. Manthey, L. Huang, M. A. Behlke and J. A. Walder, *Biochemistry*, 2004, **43**, 3537–54.
- 15 A. W. Peterson, L. K. Wolf and R. M. Georgiadis, *J. Am. Chem. Soc.*, 2002, **124**, 14601–14607.
- 16 J. SantaLucia and D. Hicks, *Annu. Rev. Biophys. Biomol. Struct.*, 2004, **33**, 415–40.
- 17 I. I. Cisse, H. Kim and T. Ha, *Nat. Struct. Mol. Biol.*, 2012, **19**, 623–7.
- 18 I. I. Cisse, H. Kim and T. Ha, *Nat. Struct. Mol. Biol.*, 2012, **19**, 623–7.
- 19 F. Manyanga, M. T. Horne, G. P. Brewood, D. J. Fish, R. Dickman and A. S. Benight, *J. Phys. Chem. B*, 2009, **113**, 2556–2563.
- 20 D. S. Dandy, P. Wu and D. W. Grainger, *Proc. Natl. Acad. Sci. U. S. A.*, 2007, **104**, 8223–8.
- 21 N. F. Dupuis, E. D. Holmstrom and D. J. Nesbitt, *Biophys. J.*, 2013, **105**, 756–66.
- 22 R. Levicky and A. Horgan, *Trends Biotechnol.*, 2005, **23**, 143–9.
- 23 A. Halperin, A. Buhot and E. B. Zhulina, *Biophys. J.*, 2005, **89**, 796–811.
- 24 A. W. Peterson, *Nucleic Acids Res.*, 2001, **29**, 5163–5168.
- 25 Y. Gao, L. K. Wolf and R. M. Georgiadis, *Nucleic Acids Res.*, 2006, **34**, 3370–7.
- 26 D. Irving, P. Gong and R. Levicky, *J. Phys. Chem. B*, 2010, **114**, 7631–40.
- 27 M. Kastantin and D. K. Schwartz, *Small*, 2013, **9**, 933–41.
- 28 V. Chan, D. J. Graves and S. E. McKenzie, *Biophys. J.*, 1995, **69**, 2243–55.
- 29 M. Shchepinov, *Nucleic Acids Res.*, 1997, **25**, 1155–1161.

- 30 A. B. Steel, R. L. Levicky, T. M. Herne and M. J. Tarlov, *Biophys. J.*, 2000, **79**, 975–81.
- 31 F. Yu, D. Yao and W. Knoll, *Nucleic Acids Res.*, 2004, **32**, e75.
- 32 B. P. Nelson, T. E. Grimsrud, M. R. Liles, R. M. Goodman and R. M. Corn, *Anal. Chem.*, 2001, **73**, 1–7.
- 33 U. Rant, K. Arinaga, S. Scherer, E. Pringsheim, S. Fujita, N. Yokoyama, M. Tornow and G. Abstreiter, *Proc. Natl. Acad. Sci. U. S. A.*, 2007, **104**, 17364–9.
- 34 T. Liebermann, W. Knoll, P. Sluka and R. Herrmann, *Colloids Surfaces A Physicochem. Eng. Asp.*, 2000, **169**, 337–350.
- 35 D. J. Fish, M. T. Horne, G. P. Brewood, J. P. Goodarzi, S. Alemayehu, A. Bhandiwad, R. P. Searles and A. S. Benight, *Nucleic Acids Res.*, 2007, **35**, 7197–208.
- 36 L. Ramdas, K. Coombes, K. Baggerly, L. Abruzzo, W. E. Highsmith, T. Krogmann, S. Hamilton and W. Zhang, *Genome Biol.*, 2001, **2**, research0047.1–research0047.7.
- 37 S. Draghici, P. Khatri, A. C. Eklund and Z. Szallasi, *Trends Genet.*, 2006, **22**, 101–9.